Caspian Journal of Applied Sciences Research, 2(AICCE'12 & GIZ' 12), pp. 182-189, 2013
Available online at http://www.cjasr.com
ISSN: 2251-9114, ©2012 CJASR

AWAM International Conference on Civil Engineering & Geohazard Information Zonation

Surface Moisture Content Retrieval from Visible/Thermal Infrared Images and Field Measurements

Abdalhaleem Abdalla HASSABALLA[1], Abdul Nasir Bin MATORI[2*], Helmi Zulhaidi bin Mohd SHAFRI[3]

[1]Civil Eng.Universiti Teknologi Petronas.Bandar Sri Iskandar, Malaysia
[2]Civil Eng. Universiti Teknologi Petronas, Sri Iskandar, Malaysia
[3]Civil Eng. Universiti Putra Malaysia, Serdang Malaysia

In this study, NOAA/AVHRR satellite was used to estimate the surface temperature and satellite estimated soil moisture content as input parameters leading to estimate the evapotranspiration over Perak Tengah & Majung regions in Malaysia. At this stage of the study, the work was focused on the analysis of soil moisture content θ and surface temperature Ts data acquired from in-situ measurements over two locations: Sitiawan and University PETRONAS UTP weather stations represents urban area and multiple land cover area respectively. Throughout the study area, θ was measured using soil moisture probe for Sitiawan and the oven method for UTP; while Ts data measured using mini thermometers for both stations. Both Ts and θ were measured in three different near surface depths 5 cm, 10 cm and 15 cm, the θ values were then plotted against Ts in graphical representations to study the impact of surface temperature on wet soils behavior. A reasonable negative relationship was noticed among the θ - Ts representation, the relation was agreed with the so called " Universal Triangle" method which is being used in the study of soil moisture, vegetation cover and temperature interaction, particularly over areas with biomass cover. Soil moisture estimation algorithm has been generated upon the "Universal Triangle" method from the satellite extracted surface temperature, Normalized Difference Vegetation Index NDVI and the field measured moisture content. Moisture content parameters were calculated, and then the moisture content algorithm was generated accordingly for the two study locations with three different "Split-window" algorithms and finally a spatial validation of satellite θ algorithms was conducted for accuracy assessment.

Key words: Surface Moisture Extraction, Satellite Surface Temperature, NOAA/AVHRR, Universal Triangle and Perak Tengah and Manjung.

1. INTRODUCTION

There have been considerable advances in the estimation of land surface environmental conditions from satellite observations, particularly from thermal infrared remote sensing data (Running and Nemani, 1988; Carlson et al., 1994). Traditionally, ground-based meteorological observations have been used in biospheric and hydrologic modeling. Satellites provide higher spatial resolution data over the entire earth and are especially important over isolated locations where meteorological observations are spare. Soil moisture is one of the few directly observable hydrologic variables that play an important role in water and energy budgets necessary for climate studies. Surface soil moisture is an important link between the surface and the atmosphere, directly influencing the exchange of head and moisture between these two sinks (Jackson and Schmugge, 1995). Further, it influences meteorological and climatic processes (Burman, 2003; Chanzy, 2003). At medium scales, it determines hydrological and agronomic processes such as runoff generation (Jackson, 1980; Loughlin, 1986; Georgakakos and Baumer, 1996; Kirkby, 2001), and evapotranspiration, crop development or irrigation needs (Wetzel And J. T, 1987; Quesney 2000; Troch et al., 2003). Surface soil moisture also influences soil erosion processes such as gully and rill erosion and head cut appearance (Montgomery And Dietrich, 1988; Moore et al., 1988; Casal et al., 1999; Kirkby, 2001; Romkens et al., 2001) or landslide occurrence. At small scales, it exerts a high influence on biogeochemical processes such as pollutant migration and, as a result, it is related to water quality issues (Famiglietti et al., 1999; Huisman et al., 2002). Soil moisture variations normally follow rainfall trends.

However, soil moisture is often somehow difficult

to measure accurately in both time and space, especially at large scales. Most of the soil moisture measuring methods which have become established consist of point- based probes which require the application of complex geostatistical techniques to obtain estimates over fields or large areas (Kachanoski et al., 1988) in addition, the high spatial and temporal variability of soil moisture makes it difficult to extrapolate from point-based measurements to larger scales.

This paper is aiming at (1) retrieving Ts from satellite images using NDVI and surface emissivity ε for Perak Tengah region through three different algorithms of the split-window method which is being used widely in Ts retrieval, and then (2) producing corrected satellite Ts through holding is-situ measured Ts, finally, (3) to generate corrected surface θ algorithm for the study area.

1.1. The study area

Perak Tengah & Manjung are part of Perak state lay between latitude $4^o00` - 4^o30`$ N and longitude $100^o30` - 101^o00`$ E (fig.1), with an area of 2,400 square kilometers. NOAA/AVHRR satellite images over the study area (through June-August 2009) were acquired and used for satellite estimated Ts rectification. Further, NOAA/AVHRR 17&18 images (from February − April 2011) have been acquired for θ algorithms generation. Five stations were selected throughout the study area in terms of the variety in the environment and vegetation cover explained as Sitiawan to represent impervious surfaces, Pusat Pertanian Titi Gantong represents the agricultural lands, Mardi Parit & UTP represent a mixed surface cover type and Pusat Pertanian Lekir represents forests cover.

2. MATERIALS AND METHODS

2.1. Split-window algorithm for deriving Ts

In order to process the acquired AVHRR images for surface temperature extraction, subset area has been delineated surrounding each weather station and any spatial computation performed within each subset area was assumed to represent the average value of the sub area pixels. On the other hand, in-situ measurements of Ts and θ were done using mini thermometer and a NETRON 740 soil moisture probe respectively. The general form of the split-window equation can be written as:

$$Ts = T_4 + A(T_4 - T_5) + B \quad (1)$$

Where:

Ts represents the land surface temperature, T_4 and T_5 represent the brightness temperature for channel 4 and 5 respectively, A and B are the coefficients determined by the impact of atmospheric conditions and other related factors on the thermal spectral radiance and its transmission in channels 4 and 5.

Using the parameters A_0, P and M given by (Becker and Li, 1990) proposed a simplified algorithm with the two coefficients A and B as:

$$A = (M - P)/2 \quad (2)$$

$$B = A_0 + T_4(P - 1) \quad (3)$$

Where the parameters A_0, P and M have been calculated by Becker (Becker and Li, 1990) as:

$$A_0 = 1.274$$

$$P = 1 + 0.15616\frac{(1-\varepsilon)}{\varepsilon} - 0.482\frac{\Delta\varepsilon}{\varepsilon} \quad (4)$$

$$M = 6.26 + 3.98\frac{(1-\varepsilon)}{\varepsilon} + 38.33\frac{\Delta\varepsilon}{\varepsilon} \quad (5)$$

Using Sobrino (Sobrino et al., 1993) formula:

$$Ts = T_4 + 1.06(T_4 - T_5) + 0.46(T_4 - T_5)^2 + 53(1-\varepsilon_4) - 53\Delta\varepsilon \quad (6)$$

Ts Estimation by Uliveri (Ulivieri et al., 1994):

$$T = T_4 + 1.8(T_4 - T_5) + 48(1-\varepsilon) - 75\Delta\varepsilon \quad (7)$$

2.2. NDVI

The NDVI measurements were made with a combined red and near-infrared radiometer, developed at the NASA/Goddard Space Flight Centre, which measures the reflected radiation in the bands (0.58-0.68 μm) and (0.73-1.1 μm) 8:

$$NDVI = \frac{NIR - RED}{NIR + RED} \quad (8)$$

2.3. Surface emissivity ε

Emissivity was estimated via an empirical algorithm based on the relationship between

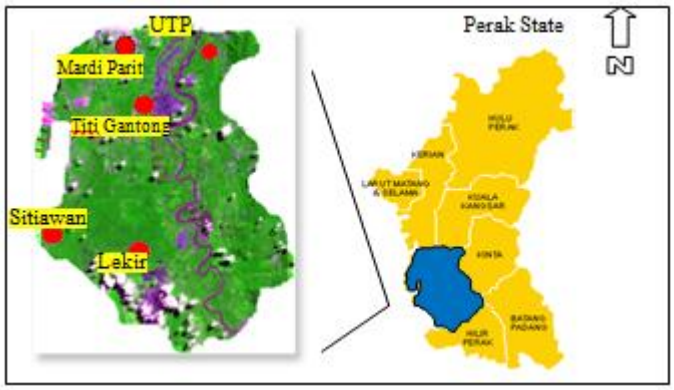

Fig. 1: Perak Tengah & Manjung area, the study areas are shown in the inset.

emissivity and the logarithm of NDVI (Van De Griend and Owe, 1993) in the range [0.955- 0.985 µm]. The emissivity of channel 4, ε4, The emissivity of channel 5, ε5 and the emissivity difference of channels 4 and 5, ε4 − ε5 (Δε), are as follows 9 and 10 and and 11and 12 :

$$\varepsilon_4 = 0.9897 + 0.029\,Ln(NDVI) \quad (9)$$

$$\Delta\varepsilon = 0.01019 + 0.01344\,Ln(NDVI) \quad (10)$$

$$\varepsilon_5 = \varepsilon_4 - \Delta\varepsilon \quad (11)$$

$$\varepsilon = 0.5(\varepsilon_4 + \varepsilon_5) \quad (12)$$

2.4. Soil Moisture Estimation

A simple regression relationship between θ, Ts and NDVI to predict the soil moisture profile from near-surface measurements through different soil depths is achieved according to the Universal Triangle theorem which explains that "there is a unique relationship among soil moisture, vegetation cover, and surface temperature for a given region (Carlson et al., 1994; Gillies et al., 1997)". The results of the developed model were later confirmed by theoretical studies using the Soil-Vegetation-Atmosphere Transfer SVAT model. Figure 2 represents a schematic description of the relationship sometimes referred to as the 'Universal Triangle' (Zhan et al., 2002).

2.5. θ, NDVI* and Ts* relationship

(Carlson et al., 1994) found that the relationship between soil moisture θ, NDVI*, and Ts* can be expressed through a regression formula such as:

$$\theta = \sum_{i=0}^{i=n}\sum_{j=0}^{j=n} a_{ij}\mathrm{NDVI}^{(i)}T^{(j)} \quad (13)$$

In terms of a second order polynomial, the above equation can be expanded as:

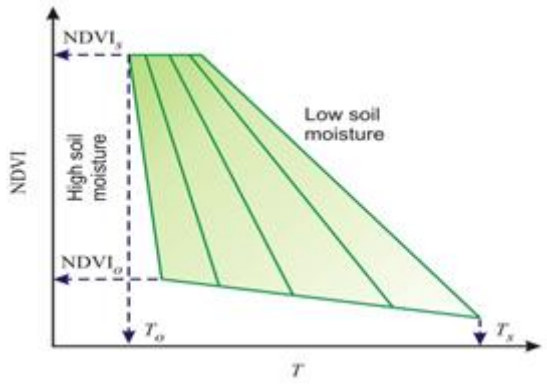

Fig. 2: Universal Triangle indicating relationship between soil moisture, temperature and NDVI

$$\theta = a_{00} + a_{10}NDVI^{*} + a_{20}NDVI^{*2} + a_{01}T^{*} + a_{02}T^{*2} + a_{11}NDVI^{*}T^{*} + a_{22}NDVI^{*2}T^{*2} + a_{12}NDVI^{*}T^{*2} + a_{21}NDVI^{*2}T^{*} \quad (14)$$

Where

$$T^{*} = \frac{T - T_o}{T_s - T_o} \quad (15)$$

$$NDVI^{*} = \frac{NDVI - NDVI_o}{NDVI_s - NDVI_o} \quad (16)$$

Ts and NDVI are observed land surface temperature and normalize difference vegetation index, respectively, and the subscripts o and s stand for minimum and maximum values.

3. RESULTS AND DISCUSSION

3.1. Satellite corrected Surface Temperature Ts

Among the four different parts of the study area, UTP station was selected as sample study in this paper for the representation and the clarification of how satellite Ts used in conjunction with in-situ measured Ts and θ achieved at two depths at surface 5 cm and 10 cm, besides NOAA/AVHRR 17 images were used. The values of satellite surface temperature extracted from the images were rectified through applying a linear regression sketch with measured surface temperatures taken in-situ in the same time of images acquisition. Figures 3 and 4 show the relationships between the two surface temperature sets for UTP location. The resultant corrected Ts was then used beside NDVI and field measured θ resulted in moisture parameters generation (equation 14), for each of the three split-window Ts.

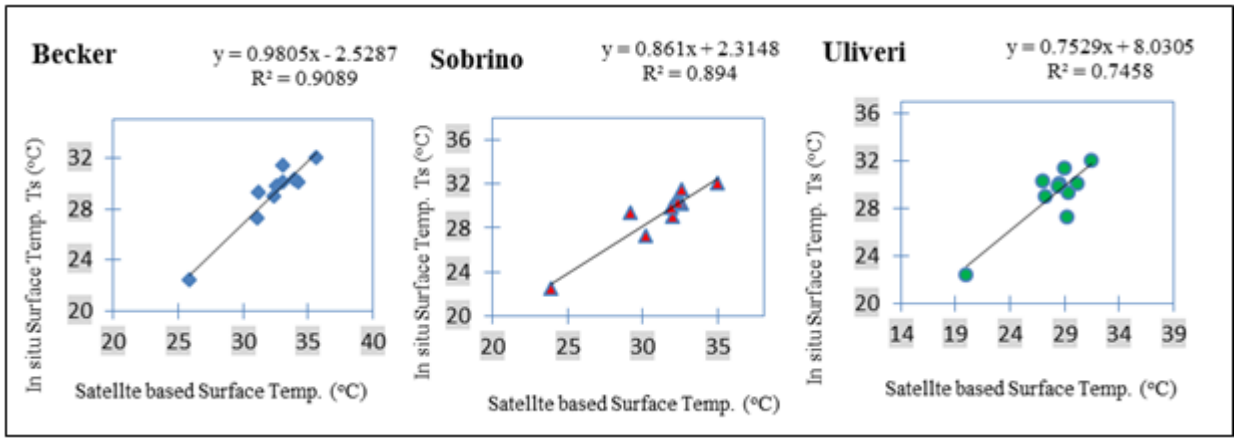

Fig. 3: Correlation between soil surface temperature measured on field and satellite based surface temperature for temperature correction, using 3 different split-window techniques applied at depth 5 cm over UTP location.

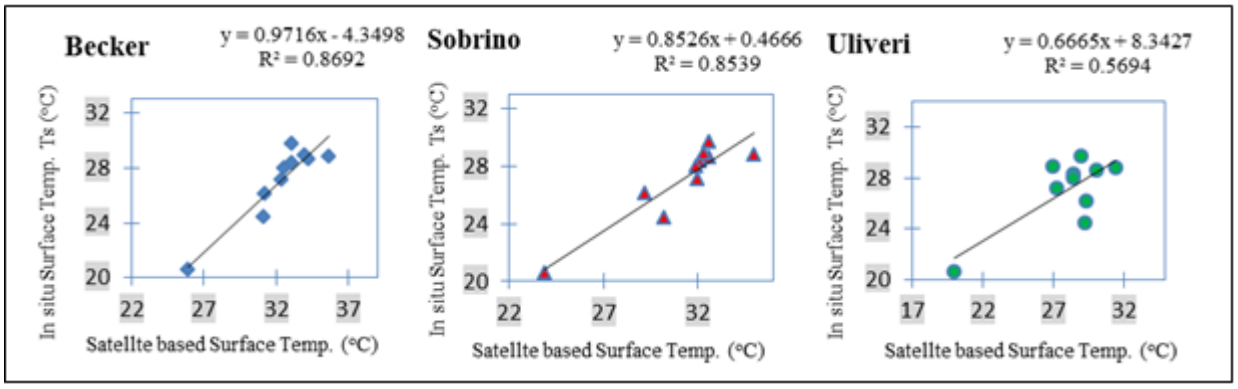

Fig. 4: Correlation between soil surface temperature measured on field and satellite based surface temperature for temperature correction, using 3 different split-window techniques applied at depth 10 cm over UTP location.

Table 1 below shows the resulted regression approach parameters calculated from Equation (14) for multiple surface cover types represented by UTP location. The in-situ measured moisture content has been taken at depths 5 cm and 10 cm.
A moisture content map was generated benefiting from parameters of daily moisture content measured in-situ at 5 cm and 10 cm depths in conjunction with the acquired NOAA 17 satellite images in overpass times; this map is a sort of raster image produced by ArcGIS software in which each pixel represents a value of moisture content. In this study also LANDSAT ETM+ image acquired in July 20, 2001 has been used for moisture map representation because of its relative high spatial resolution (Figure 5), thus these maps availed concise representations of surface moisture content distribution over the study area.

3.1. Ts-NDVI relationship

The study was directed to examine the effect of land surface temperature and its role in assessing the surface moisture statement within the selected two depths of corrected Ts, 5 cm as top soil surface and 10 cm as middle surface during satellite overpass time over UTP location while, NDVI was extracted directly the same images as well.

A good negative correlation was found between NDVI and satellite corrected Ts over the study area during NOAA 17 overpass time (first reading), resulting a typical Universal Triangle which was introduced earlier. In which the vegetation radiometric temperature is always close to air temperature, but the surface radiant temperature over bare soil can vary depending on the soil water content.

Figure 6 shows a typical universal triangle composed using a scatterplot of TS and NDVI which is seen on the left image (grey colour). The colours given on the right image refer to the soil surface moisture distribution in which: The green colour (cluster 1) denotes a dense vegetation areas, represented by relatively low Ts, while the yellow colour (cluster 2) denotes a fully wetted soil surface which covers areas surrounding water bodies and represented graphically with very low Ts (almost Y-axes). Finally, the grey colour (cluster 3) takes place over urban areas and represented graphically with scattered points and high Ts.

Table 1: Satellite Corrected Parameters For UTP Location

Algorithm	M C measuring depth	M C parameters								
		a00	a10	a20	a01	a02	a11	a22	a12	a21
Becker	At 5 cm depth	1.61	-6.85	6.23	3.23	-4.77	0.33	1.12	4.59	-5.04
	At 10 cm depth	-1.00	-1.48	2.89	3.11	0.15	9.03	-3.88	-9.05	-9.38
Sobrino	At 5 cm depth	-45.56	106.81	-61.92	23.39	-42.73	-2.42	-36	87.31	-38.73
	At 10 cm depth	11.36	-33.38	24.50	0.86	-10.90	7.35	-1.30	12.51	-10.54
Uliveri	At 5 cm depth	4.65	-12.50	6.71	-3.37	-2.87	10.72	-6.38	6.40	-3.50
	At 10 cm depth	285.97	-1786	0.0018	869	-939.8	332.1	697.6	632.7	-1789

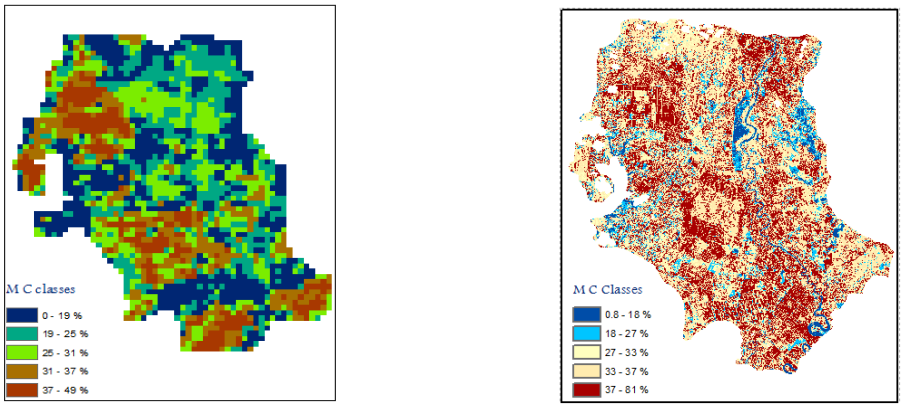

Fig. 5: The generated surface moisture map of the study area from sensors NOAA 17(left) and LANDSAT ETM+ (right).

3.2. Algorithm Validation

In order to examine the accuracy of the generated surface moisture content algorithms, a sort of spatial validation was implemented in terms of comparing the generated surface moisture map to a land use/cover map of the study area (Figure 7). The validation came out with considerable notices, most of the areas which are covered by vegetation in the land use/cover map meet the highest value of θ from generated map, which vary between 0.33 to 0.81 followed by forest areas with θ range of 0.27 to 0.33 finally, the least θ values noticed over the urban areas and fallow lands, this could be attributed to canopy resistance to latent heat flux (Smith and Choudhury, 1990; Smith and Choudhury, 1991; Carlson et al., 1994). This implies that the spatial variation in surface radiant temperature will be small over full vegetation cover. The agreement in the visual representation between the θ map with corrected Ts and the land use reflects to some extent the accuracy of the used algorithm in estimating θ at surficial level, particularly in case of landscape and regional scales.

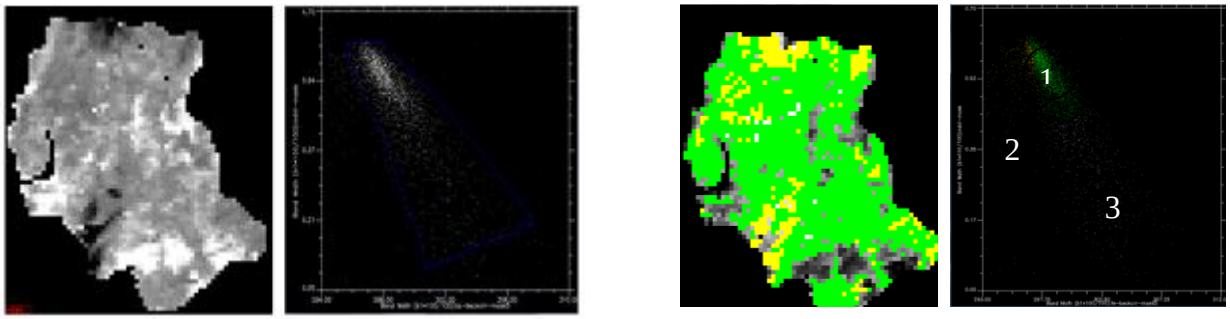

Fig. 6: Satellite Corrected Ts- NDVI relationship for depth of measurements 5 cm using Becker algorithm.

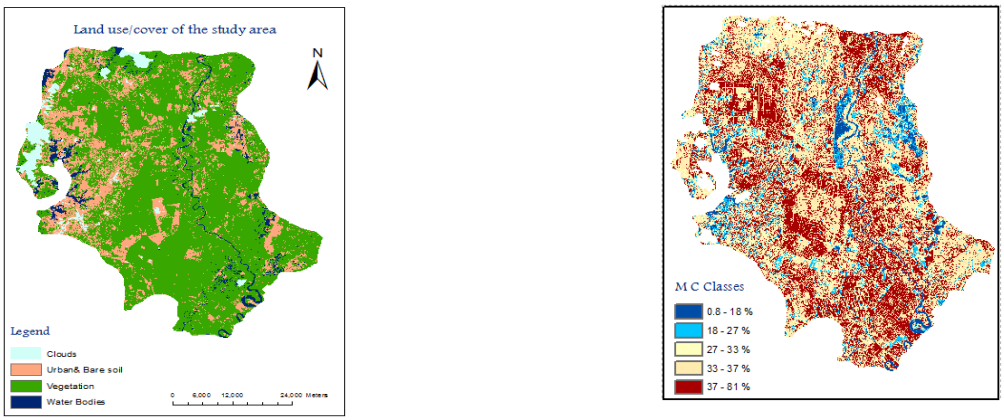

Fig. 7: spatial validation of moisture generated map (right) using land use image (left).

4. CONCLUSION

The satellite based corrected surface temperature achieved reasonable results in surface moisture content estimation, especially over agricultural area and areas with a uniform cover, this can be justified as: the low thermal mass of green canopy enhances the surface moisture availability. Throughout the study, the objectives bellows were done:

- In-situ measurements of soil moisture were achieved in two variable depths 5 cm and 10 cm and used in a regression equation with corrected Ts and NDVI to generate moisture content parameters which were then used to produce surface moisture map.
- NDVI-Ts relationship was plotted to study the impact of vegetation and surface covers status in Ts and θ assessment in which, a strong negative correlation was found between NDVI and Ts especially over vegetated and uniform cover areas. On the other hand bare soils and built-up areas witness abnormality in TS-NDVI relationship; this must be due to the homogeneous cover as well as the variation of estimated Ts over those areas due to the surface emission effect shared by traffic, machines and /or impervious surfaces over urban areas.

Finally, surface moisture content algorithms was validated spatially by comparing the surface moisture boundaries to the surface cover type of land use map over the study area generated using maximum likelihood classification in which a landsat ETM+ image was used for more accuracy and clarification.

REFERENCES

Becker F., Li Z. L (1990). Towards A Local Split Window Method over Land Surface. International Journal of Remote Sensing, 3: 369-393.

Burman R. D (2003). Evapotranspiration Formulas. In: Encyclopedias of Water Science. Stewar B A; Howell T. A, EDS, Marcel Dekker, USA, 253–257.

Carlson T., Gillies R., and Perry E (1994). A method to Make use of Thermal Infrared Temperature and NDVI Measurements to Infer Surface Soil Water Content and Fractional Vegetation Cover. Remote Sensing Review, 9: 161-173.

Casal J. ; Lopez J. J. And Gira Ldez J. V (1999). Ephemeral Gully Erosion in Southern Navarra. Spain. Catena, 36: 65–84.

Chanzy A (2003). Evaporation From Soils. In: Encyclopaedia of Water Science. Stewar B A; Howell T A, EDS, Marcel Dekker, USA, 249–251.

Famiglietti J. S.; Devereaux J. A.; laymon C. A.; Tsegaye T.; Houser P. R.; Jackson T. J.; Graham S. T.; Rodell M. And Van Oevelen P. J (1999). Ground based Investigation of Soil Moisture Variability Within Remote Sensing Footprints During the SGP 97 Hydrology Experiment. Water Resources Research , 35: 6, 1839–1851.

Georgakakos K. P., and Baumer O. W (1996). Measurement and Utilization of On-Site Soil Moisture Data. Journal of Hydrology, 184: 131–152.

Gillies R.; Carlson T.; Kustas W., and Humes K (1997). A Verification of the "Triangle" Method for Obtaining Surface Soil Water Content and Energy Fluxes from Remote 140 Measurements of the Normalized Difference Vegetation Index (NDVI) and Surface Radiant Temperature. Int. J. Remote Sens. 18: 3145-3166.

Huisman J. A.; Snepvangers J.; Bouten W. And Heuvelink G. B (2002). Mapping Spatial Variation in Surface Soil Water Content: Comparison of Ground-Penetrating Radar and Time Domain Reflectometry. Journal of Hydrology, 269: 194–207

Jackson T. J (1980). Profile Soil Moisture From Surface Measurements. Journal of Irrigation and Drainage Division Proceedings, 106: 81–92.

Jackson T. J. and Schmugge T. J (1995). Surface Soil Moisture Measurement With Microwave Radiometry. Elsevier Science LTD. Printed in Great Britain, Acta Astronautica, 35: 477-482.

Kachanoski R. G.; Gregorich E. G. And Van Wesenbeeck I. J (1988). Estimating Spatial Variations of Soil Water Content Using Noncontacting Electromagnetic Inductive Methods. canadian Journal of Soil Science, 68: 715–722.

Kirkby M. J (2001). Modelling the Interactions between Soil Surface Properties and Water Erosion. Catena, 46: 89–102.

Loughlin E. M. O (1986). Prediction of Surface Saturation Zones in Natural Catchments by Topographic Analysis. Water Resources Research, 22: 5, 794–804.

Montgomery D. R. And Dietrich W. E (1988). Where do Channels Begin. Nature, 336: 232–234.

Moore I. D.; Burch G. J. And Mackenzie D. H (1988). Topographic Effects on The Distribution of Surface Soil Water and The Location of Ephemeral Gullies. Transactions of The Asae, 31: 1098–1107.

Quesney A.; Garat-Mascle S. Le He´;Taconet O.; Vidal-Madjar D.; Wigneron J. P.; Loumagne C., and Normand M (2000). Estimation of Watershed Soil Moisture Index from ERS/SAR Data. Remote Sensing of Environment, 72: 3, 290–303.

Romkens M. J. M.; Helming K. And Prasad S. N (2001). Soil Erosion Under Different Rainfall Intensities, Surface Roughness and Soil water Regimes. Catena, 46: 103–123.

Running S. W., and Nemani R. R (1988). Relating Seasonal Patterns of The AVHRR Vegetation Index to Simulated Photosynthesis and Transpiration of Forests in Different Climates. Remote Sen. Environ. 24: 347-67.

Smith R. C. G., and Choudhury B. J (1990). On the Correlation of Indices of Vegetation and Surface Temperature over South Eastern Australia. Int. J. Remote Sens., 11: 2113-2120.

Smith R. C. G., and Choudhury B. J (1991). Analysis of Normalized Difference and Surface Temperature Observations over Southeastern Australia. Int. Remote Sens., 12: 2021-2044.

Sobrino J. A., Li Z. L., Stall M. P., and Becker F (1993). Impact of the Atmospheric Transmittance and Total Water Vapour Content in The Algorithms for Estimating Sea Surface Temperature. IEEE Trans. Ceosci. Remote Sens. 31: 946-958.

Troch P. A.; Paniconi C.; Mclaughlin D (2003). Catchment-Scale Hydrological Modeling and Data Assimilation. Advances in Water Resources, 26: 2, 131–135.

Ulivieri C., Castronouvo M. M., Francioni R., and Cardillo A (1994). A Split Window Algorithm for Estimating Land Surface Temperature from Satellites. Advances in Space Research, 3: 59-65.

Van De Griend A. A., and Owe M (1993). On the Relationship between Thermal Emissivity and the Normalized Difference Vegetation Index for Natural Surfaces. International Journal of Remote Sensing, 14: 6, 1119-1131.

Wetzel P. J. And J. T (1987). Concerning The Relationship between Evapotranspiration and Soil Moisture. Chang Journal of Climate and Applied Meteorology, 26: 18–27.

Zhan, X., Miller, S., Chauhan, N., Di, L., Ardanuy, P. And Running, S (2002). Soil Moisture Visible/Infrared Imager/Radiometer Suite Algorithm Theoretical Basis Document. Version 5.